Carcinogenesis, 2015, Vol. 36, No. 2, 272–279

doi:10.1093/carcin/bgu324
Advance Access publication January 2, 2015
Original Manuscript

ORIGINAL MANUSCRIPT

Antitumor effects of hyaluronan inhibition in desmoid tumors

Alexandra Briggs, Laura Rosenberg[1], Justin D.Buie, Hira Rizvi, Monica M.Bertagnolli and Nancy L.Cho[*]

Department of Surgery, Brigham and Women's Hospital, Boston, MA 02115, USA and [1]Department of Surgery, Massachusetts General Hospital, Boston, MA 02114, USA

[*]To whom correspondence should be addressed. Tel: +1 617 732 6830; Fax: +1 617 739 1728; Email: nlcho@partners.org

Abstract

Desmoid tumors (DTs) are rare, mesenchymal tumors that exhibit features of an abundant wound healing process. Previously, we showed that mesenchymal stem cells (MSCs) are constituents of DTs and may contribute to desmoid tumorigenesis via activities associated with wound healing. Hyaluronan (HA) is a long-charged chain of repeating glucuronate and *N*-acetylglucosamine disaccharides that is synthesized by HA synthases (HAS) and degraded by hyaluronidases (HYAL). HA is secreted into the extracellular matrix by injured stroma and is important for normal tissue repair and neoplastic progression. Here, we investigated the presence of HA in DTs and the antitumor effects of the HA inhibitor, 4-methylumbelliferone (4-MU), on DT-derived mesenchymal cells. By immunohistochemistry and enzyme-linked immunosorbent assay, we found abundant expression of HA in 29/30 DTs as well as >5-fold increased HA levels in DT-derived cell lines relative to controls. Immunohistochemistry also demonstrated high expression of HAS2 in DTs, and quantitative PCR analysis showed increased HAS2 upregulation in frozen DTs and DT-derived cells. 4-MU treatment of DT-derived cells significantly decreased proliferation as well as HA and HAS2 levels. Fluorescent immunohistochemistry showed that MSCs in DTs coexpressed HA, HAS2, HYAL2, as well as the major HA receptor CD44 and HA coreceptor TLR4. Taken together, our results suggest that paracrine regulation of HA signaling in DTs may contribute to MSC recruitment and tumor proliferation. Future studies investigating the role of HA in tumor-stroma crosstalk and inhibition of HA-MSC interactions as a novel therapeutic target in DTs and other solid tumors are warranted.

Abbreviations:

DTs	desmoid tumors
HA	hyaluronan
HDF	human dermal fibroblast
HAS	HA synthases
HYAL	hyaluronidases
4-MU	4-methylumbelliferone
MSCs	mesenchymal stem cells

Introduction

Desmoid tumors (DTs), or aggressive fibromatosis, are mesenchymal tumors with a dense, infiltrative character than can lead to significant disfigurement, functional deficits and death (1,2). Although rare in the general population, DTs are a common cause of death in patients with familial adenomatous polyposis. Treatment often involves wide surgical excision, which is associated with high recurrence rates and unresectable disease (3). Although several studies reported partial response of DTs to drug treatments and radiation therapy, effective systemic therapy remains elusive, in large part, due to the limited understanding of DT pathophysiology (4–7).

Histologically, DTs are characterized by an abundant wound healing process with features nearly indistinguishable from benign hyperproliferative conditions such as keloids and hypertrophic scars (8,9). Given that tumors are often described as 'wounds that do not heal', we hypothesize that DTs develop as

Received: July 31, 2014; **Revised:** December 10, 2014; **Accepted:** December 25, 2014

a manifestation of defective tissue repair and the inability to arrest the proliferative phase of wound healing (10). Moreoever, DTs also exhibit markers of increased angiogenesis and fibrosis, suggesting that chronic inflammation and defective wound healing resolution play significant roles in desmoid tumorigenesis (11,12).

Normal wound healing is a tightly orchestrated process mediated by inflammatory cells in response to tissue injury. Hyaluronan (HA) is a glycosaminoglycan that is produced by injured stroma and rapidly deposited in the extracellular matrix where it regulates repair processes through crosstalk with various inflammatory cells (13). The major HA ligand, CD44, is expressed as a cell surface receptor on mesenchymal stem cells (MSCs), which are multipotent cells that play a key role in wound healing (14–16). MSCs are mobilized in response to multiple paracrine and endocrine signals, such as HA, that are released during the inflammatory process (17–19). At wound sites, these pluripotent cells engraft and promote healing by executing tissue remodeling and by differentiating into endothelial cells, fibroblastss and myofibroblasts. During the resolution phase of normal wound healing, recruited stem/progenitor cells undergo terminal differentiation or apoptosis. However, under conditions of chronic inflammation or tumor progression, these activated cells persist. Previously, we showed that aberrantly activated MSCs are present in DTs and may be critical to desmoid formation (20). Similarly, Wu *et al.* (21) reported that DTs express genes and cell surface markers characteristic of MSCs and suggested that MSCs may be the progenitor cells of DTs. Other groups have demonstrated that MSC migration to injured tissue is dependent upon CD44 cell surface expression and adhesion to HA (22,23).

Based on these observations, we hypothesized that HA plays an important role in desmoid tumorigenesis through crosstalk with MSCs at sites of tissue injury. To test this idea, we examined the expression of HA in human DTs s and DT-derived cell lines. We also investigated the antitumorigenic effects of HA inhibition in DT-derived mesenchymal cells using 4-methylumbelliferone (4-MU), a HA synthesis inhibitor. Finally, we examined interactions between $CD44^+$ MSCs and members of the HA pathway. These studies are the first to investigate the presence of HA in DTs and implicate crosstalk between $CD44^+$ MSCs and HA in contributing to the etiology of DTs.

Materials and methods

Human DT samples

Human DTs and matching adjacent normal tissue were obtained from an archived tissue bank of surgical specimens resected from patients under a protocol previously approved by the institutional review board at the Brigham and Women's Hospital. A portion of the tumor was fixed in formalin and embedded in paraffin for immunohistochemical analysis. The remaining portion was snap frozen in liquid nitrogen and stored at –80°C for molecular analysis.

Desmoid cell lines

Between January 2013 and January 2014, three fresh DTs were obtained from the operating room to establish primary cell lines for *in vitro* studies. Tumors were minced in supplemented growth medium and plated on tissue culture dishes. After 24 h, the minced tumor was manipulated through a 100-µm nylon mesh cell strainer under sterile conditions, while being washed with growth medium. The wash was then centrifuged at 1500 rpm for 5 min, with the resultant pellet resuspended in growth medium and plated in 25 cm^2 tissue culture flasks. The following day, cells that were nonadherent to flasks were discarded. The remaining cells were maintained and expanded as primary desmoid-derived cell lines.

Cells were cultured and expanded in MesenPro RS™ Medium supplemented with the associated MesenPro RS™ Growth Supplement, 2 mM L-glutamine, 100 units/ml penicillin and 100 µg/ml streptomycin. Cell lines have not been tested; however, experiments were performed using early passage cells (passage 1–5) to minimize chance of cross contamination. Normal human dermal fibroblasts (HDF) were obtained from American Type Culture Collection (Manassas, VA) and cultured in Dulbecco's modified Eagle's medium containing 10% fetal bovine serum, 100 units/ml penicillin, and 100 µg/ml streptomycin. Unless otherwise indicated, cell culture reagents were purchased from Life Technologies (Grand View, NY). Cells were maintained at 37°C in a humidified incubator containing 5% CO_2. Patient characteristics of each DT-derived cell line are described in Table 1.

Immunohistochemistry

Immunohistochemistry and immunofluorescent staining were performed as previously described (20). Primary antibodies used for these experiments include the following: HABP2 (Sigma), HAS2 (Santa Cruz Biotechnology), HYAL2 (Santa Cruz Biotechnology), CD44 (Cell Signaling), TLR4 (Santa Cruz Biotechnology) and DAPI (Life Technologies). All primary antibodies were diluted at 1:100 in Antibody Diluent Reagent Solution (Invitrogen) and reactions carried out overnight at 4°C.

Enzyme-linked immunosorbent assay (ELISA)

Cells were plated in six-well plates at a concentration of 200 000 cells per well in normal growth medium, and incubated overnight at 37°C in a humidified incubator containing 5% CO_2. To obtain baseline expression of HA levels, on the following day normal growth medium was replaced with serum-free Dulbecco's modified Eagle's medium. Thirty-six hours after the medium was replaced, this replaced medium was aspirated and collected. The cells were harvested with trypsin and counted using a hemocytometer. The collected medium was used to assay for HA levels using the Hyaluronan Quantikine ELISA kit from R&D Systems (Minneapolis, MN), which was performed according to manufacturer protocol. Medium from each cell line was assayed in triplicate. Final HA levels were corrected according to the results of the final cell count from the day of medium collection.

To observe the effect of 4-MU on HA levels in different cell lines, the same protocol as above was performed, seeding 200 000 cells per well of a six-well plate. However, when the medium was replaced the day after seeding, this medium was replaced with either control (dimethyl sulfoxide only) or treated medium (0.4 mM 4-MU). This medium was aspirated and collected 36 h later, at which time cells were harvested and counted. This medium was then used to perform the HA ELISA as above. Each sample was assayed in triplicate, and final HA levels were again corrected according to the results of the final cell count.

Table 1. Patient characteristics

Patient	Cell line	Age	Sex	Location	FAP	Primary surgery?	Prior systemic therapy?	Tumor size (cm)
1	DTS5	34	F	ABD	No	No	Liposomal doxorubicin	9.8 × 8.8 × 7.0
2	DTS6	54	M	MES	No	No	None	3.5 × 2.9 × 2.9; 1.2 × 0.9 × 0.9; 2.5 × 2.0 × 1.4, 1.3 × 1.2 × 1.0
3	DTS7	57	F	ABD	No	Yes	Celecoxib	2.5 × 2.2 × 2.0

ABD, abdominal; MES, mesentery; FAP, familial adenomatous polyposis.

Proliferation assay

Cells were plated in 96-well plates at a concentration of 2000 cells per well in normal growth medium, and incubated overnight at 37°C in a humidified incubator containing 5% CO_2. On the following day, control or treated medium was added to wells. For treated cells, 4-MU (Sigma-Aldrich Corporation, St. Louis, MO) was dissolved in dimethyl sulfoxide to make a stock solution, and serial dilutions of this stock were prepared in growth medium, ranging from concentrations between 0.1 and 2 mM, with a concentration of dimethyl sulfoxide not exceeding 1% of the final concentration. Each concentration was assayed in triplicate. Treated cells were incubated for an additional 72 h. Proliferation was determined using the CellTiter 96® AQ_{ueous} Non-Radioactive Cell Proliferation Assay kit from Promega Corporation (Madison, WI) according to the manufacturer's instructions. Briefly, after treatment, assay mix was added to each well (20 µl/well), and the plate was incubated at 37°C for an additional 4 h. The absorbance of each individual well was then determined at 490 nm. A percentage of proliferation was determined by dividing the absorbance values of the treated wells by the absorbance values of the untreated wells.

RNA extraction

RNA was extracted from frozen human tissue samples using the Aurum™ Total RNA Fatty and Fibrous Tissue Kit (Bio-Rad). RNA extracted from DT cell lines was performed using the Aurum™ Total RNA Mini Kit (Bio-Rad) per the manufacturer's instructions. The extracted RNA was eluted in a total volume of 80 µl of elution buffer and stored and –80°C. RNA concentration (ng/µl) was measured using the p300 NanoPhotometer™ (Implen).

Quantitative RT-PCR

Quantitative real time PCR (qRT-PCR) was carried out using the Brilliant III Ultra-Fast SYBR® Green QPCR Master Mix (Agilent Technologies) on the Stratagene Mx3000P qPCR system (Agilent Technologies). Amplification was carried out in 20 ul reaction mixtures containing 300 nm of specific primers for HAS2 (Forward: CAGAATCCAAACAGACAGTTC, Reverse: TAAGGTGTTGTGTGTGACTG), GAPDH (Forward: GCTCTCCAGAACATCATCTGCC, Reverse: CGTTGTC ATACCSGGAAAGAGCTT), 100 ng of total RNA, 0.2 µl 100 mM dithiothreitol, 0.3 µl diluted (1:500) reference dye, 1 µl RT/RNase block and 10 µl 2× SYBR Green QRT-PCR master mix. The reaction was performed for 10 min at 50°C, 3 min at 95°C and 40 cycles each of a 20-s dissociation step performed at 95°C and an amplification step performed at 59°C for 20 s. A melt curve analysis was performed to assess primer specificity.

The $2^{-\Delta\Delta ct}$ method of relative quantification was used to determine the fold differences in gene expression between human DT samples and normal tissue samples. This method was also used to determine the fold changes in gene expression in DT cell lines following treatment with 4-MU. GAPDH was used as the reference housekeeping gene in the analysis. Target gene threshold cycle (C_T) value was normalized to values obtained for GAPDH in the same samples. C_T values were further normalized to the average normal C_T value for tissue samples and the average untreated desmoid cell line C_T value for cell lysates. The fold change was then determined using the $2^{-\Delta\Delta ct}$ method.

Statistical analysis

Means and standard deviations were calculated for each experiment. Student's *t*-test was performed to evaluate differences between each experimental condition ($P < 0.05$ was considered statistically significant).

Results

Human DTs express hyaluronan

The presence of HA in DTs has not been determined previously. To investigate the expression of HA in DTs, we performed immunohistochemistry on 30 archived paraffin-embedded tumor specimens and 5 matched normal adjacent tissues. Tumors were obtained from patients with both sporadic and inherited forms of the disease. We found positive HA staining in 29 of 30 tumor specimens; in contrast, staining for HA in normal tissue demonstrated negative results (Figure 1A and B). Similarly, we performed ELISA on early passage cells to determine HA levels in three separate DT-derived cell lines. Cells were isolated and expanded from tumors obtained from patients immediately upon surgical resection, as previously described (20). Our results show significantly increased HA levels in all DT-derived cells relative to HDF controls (Figure 1C). HA levels were at least 5-fold greater in DT-derived cells compared to control fibroblasts and up to 30-fold higher in DTS6, a cell line obtained from a sporadic tumor located in the mesentery ($P = 0.004$ for DTS5 versus HDF, $P = 0.0002$ for DTS6 versus HDF and $P = 0.002$ for DTS7 versus HDF).

Measurement of hyaluronan synthase in DTs

High molecular weight HA (HMWHA) is produced by the HA synthases (HAS) 1 and 2 in response to tissue injury and is subsequently degraded by hyaluronidases (HYAL) into smaller fragments (24,25). These smaller HA fragments mediate the inflammatory and proliferative phases of wound healing and are implicated in tumor cell invasion and motility (26–29). Inhibition of HA synthases decreases proliferation, invasion and motility in a variety of tumor cell lines (30–33). Furthermore, HAS2 increases production of HMWHA and promotes tumor cell proliferation *in vitro* (34). To investigate the presence of HAS in DTs, we performed IHC for HAS2 in our archived desmoid specimens. We found abundant HAS2 staining in all archived DTs and virtually

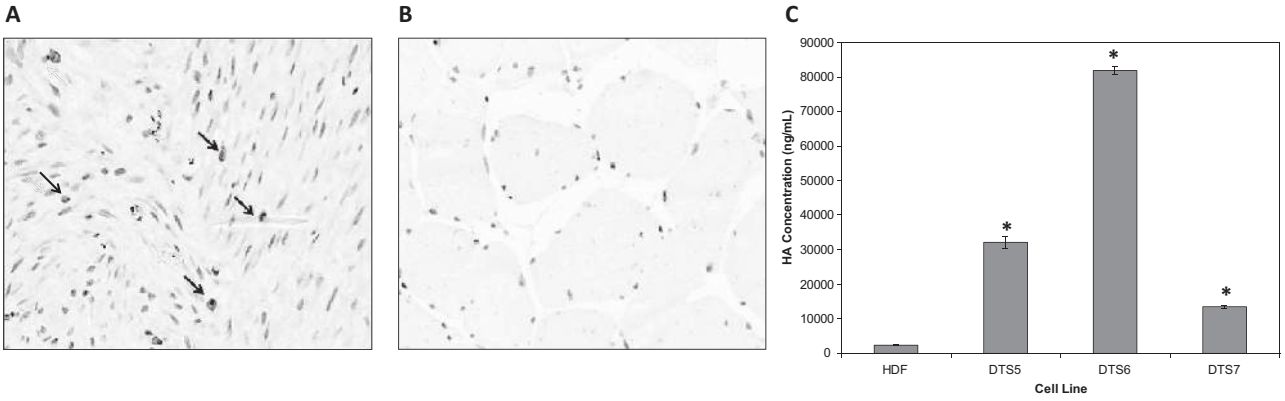

Figure. 1. Representative staining of HA in human DTs. (**A**) Thirty DT samples were stained for the HA binding protein (HABP) and demonstrated the abundant presence of HA (black arrows) within the tumors. (**B**) Matched normal tissues were negative for HA staining. Representative images were taken using an Olympus BX40 microscope at ×40 magnification. (**C**) HA ELISA was performed on three separate DT-derived cell lines and demonstrated significantly increased HA levels compared to control HDFs. Experiments were performed in triplicate and data are expressed as the mean ± SD. Asterisk indicates significant differences from HDF controls ($P < 0.05$).

no staining in matched normal tissues (Figure 2A and B). We also performed quantitative PCR on eight fresh frozen DT samples and three DT-derived cell lines. Consistent with our immunohistochemical results, we found increased upregulation of HAS2 in DTs compared to pooled matched normal tissue ($P = 0.01$) (Figure 2C). Similarly, HAS2 gene expression was increased ~2 to 4-fold in all three tumor cell lines relative to control fibroblasts (Figure 2D). While these results did not reach significance, there was a consistent trend demonstrating overall increased HAS2 expression in tumor cell lines ($P = 0.13$ for DTS5 versus HDF, $P = 0.30$ for DTS6 versus HDF and $P = 0.09$ for DTS7 versus HDF).

Antitumor activity of 4-MU in DT-derived cells

4-Methylumbelliferone is a HA synthesis inhibitor with potent anticancer properties that are primarily mediated through inhibition of HA signaling and depletion of HA precursors (33–35). To determine the effect of 4-MU on DT-derived cells, three separate cell lines were treated with varying concentrations of 4-MU (0–2 mM) for up to 72 h. As shown in Figure 3A, all three tumor cell lines demonstrated decreased proliferation in a dose-dependent manner (IC_{50} 0.4–1 mM). 4-MU also decreased HA levels in all three DT-derived cell lines following treatment with 0.4 mM for 36 h, and two of these cell lines demonstrated significant reduction ($P = 0.007$ for DTS5 versus HDF, $P = 0.01$ for DTS6 versus HDF) (Figure 3B). To investigate the effect of 4-MU on HAS2, DT-derived cells were treated with 0.4 mM of 4-MU for 36 h and demonstrated ~2-fold decrease in HAS2 gene expression ($P < 0.001$ for all treated versus untreated cell lines) (Figure 3C). Of note, 4-MU treatment demonstrated minimal effect on HA levels and proliferation in normal fibroblasts, suggesting that treatment response is limited to tumor cells.

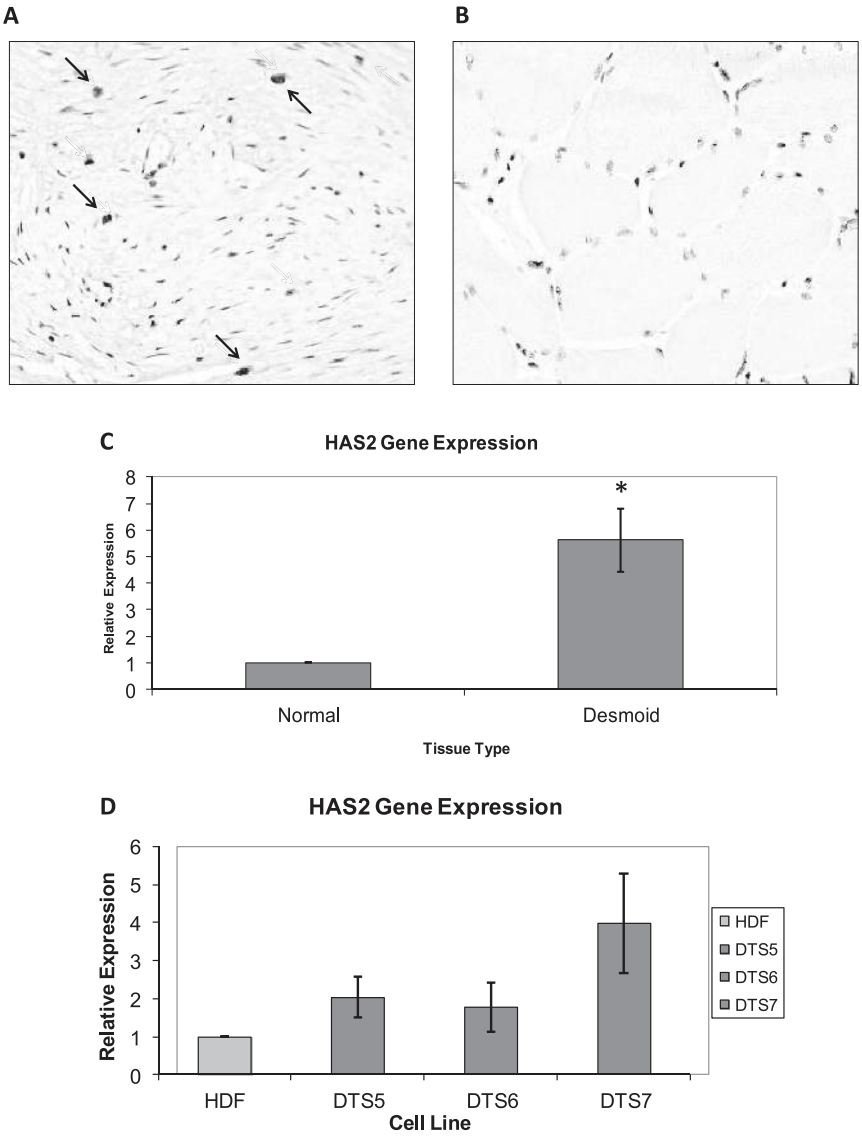

Figure 2. HAS2 expression in DTs and desmoid-derived cells. (**A**) Immunohistochemistry of paraffin-embedded DTs for HA synthase (HAS) 2 was performed and representative images show abundant HAS2 expression in DTs (black arrows). (**B**) Matched normal tissues were negative for HAS2 staining. Original magnification was ×40. (**C**) Quantitative PCR was performed on eight separate fresh frozen desmoids and relative gene expression of HAS2 was compared to a matched pool of 5 normal tissue samples. Asterisk indicates a significant difference between tumor and control tissue ($P < 0.05$). (**D**) Quantitative PCR was performed on three separate desmoid-derived cell lines and demonstrated increased HAS2 gene expression relative to control fibroblasts. Experiments were performed in triplicate and data are expressed as the mean ± SD. Asterisk indicates significant differences between tumors and controls ($P < 0.05$).

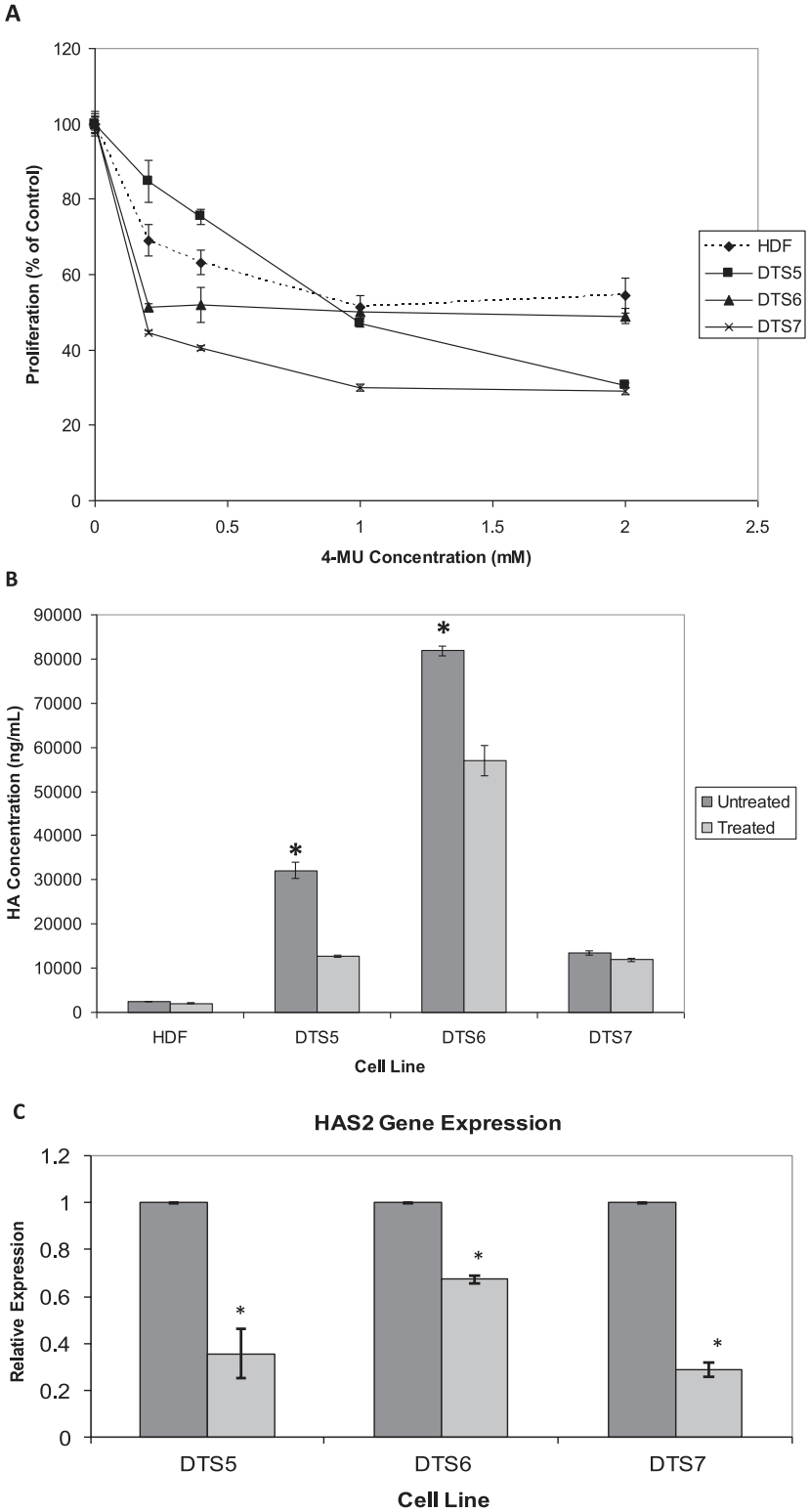

Figure 3. Effect of 4-MU in desmoid-derived cells. (**A**) Treatment with 4-MU (0–2 mM) decreased tumor cell proliferation in a dose-dependent manner. (**B**) 4-MU treatment (0.4 mM) also significantly reduced HA levels in all three desmoid-derived cell lines by ELISA compared to controls. (**C**) 4-MU treatment (0.4 mM) significantly decreased HA synthase (HAS) 2 expression in DT-derived cells. Experiments were performed in triplicate and data are expressed as the mean ± SD. Asterisk indicates significant differences from human dermal fibroblast controls ($P < 0.05$).

CD44⁺ MSCs may interact with HA in DTs

Bone marrow-derived MSCs play an important role in wound healing and tumorigenesis and are recruited in response to various chemotactic signals, including HA. Previously, we showed that CD44⁺, CD73⁺, CD90⁺ MSCs are an abundant constituent of DTs and may play an important role in promoting

desmoid tumorigenesis (20). To investigate whether MSCs in DTs may be involved in tumor-promoting interactions with HA, we performed immunofluorescence for the MSC marker and major HA receptor, CD44, and the HA-binding protein, HABP2. We found coexpression of both CD44 and HABP2 in our desmoid samples (Figure 4A). Interestingly, $CD44^+$ MSCs also coexpressed the HA-synthesizing enzyme HAS2, the HA-catabolizing enzyme HYAL2, and the HA coreceptor, TLR4 (Figure 4B–D). These results suggest that the tumorigenic effects of HA are mediated by MSCs.

Discussion

Recent studies examining the role of tumor stroma in contributing to tumor formation and chemoresistance have increased interest in targeting the stromal compartment in combination with cytotoxic agents as a dual approach to enhancing therapy in solid tumors (36). HA is a prominent component of the stromal microenvironment in a variety of cancers, and increased HA deposition is implicated in tumor invasion and progression (27–29). HA is secreted as a high-molecular weight polymer in the extracellular matrix and is subsequently degraded by hyaluronidase enzymes into smaller fragments that mediate the inflammatory and proliferative phases of wound healing. Because abundant wound healing is a hallmark of desmoid histology, we investigated the presence of HA in DTs to identify a potentially novel therapeutic target for this challenging disease. Furthermore, we speculated that HA-MSC interaction may contribute to DT etiology through recruitment of these specialized stem cells to sites of tissue injury.

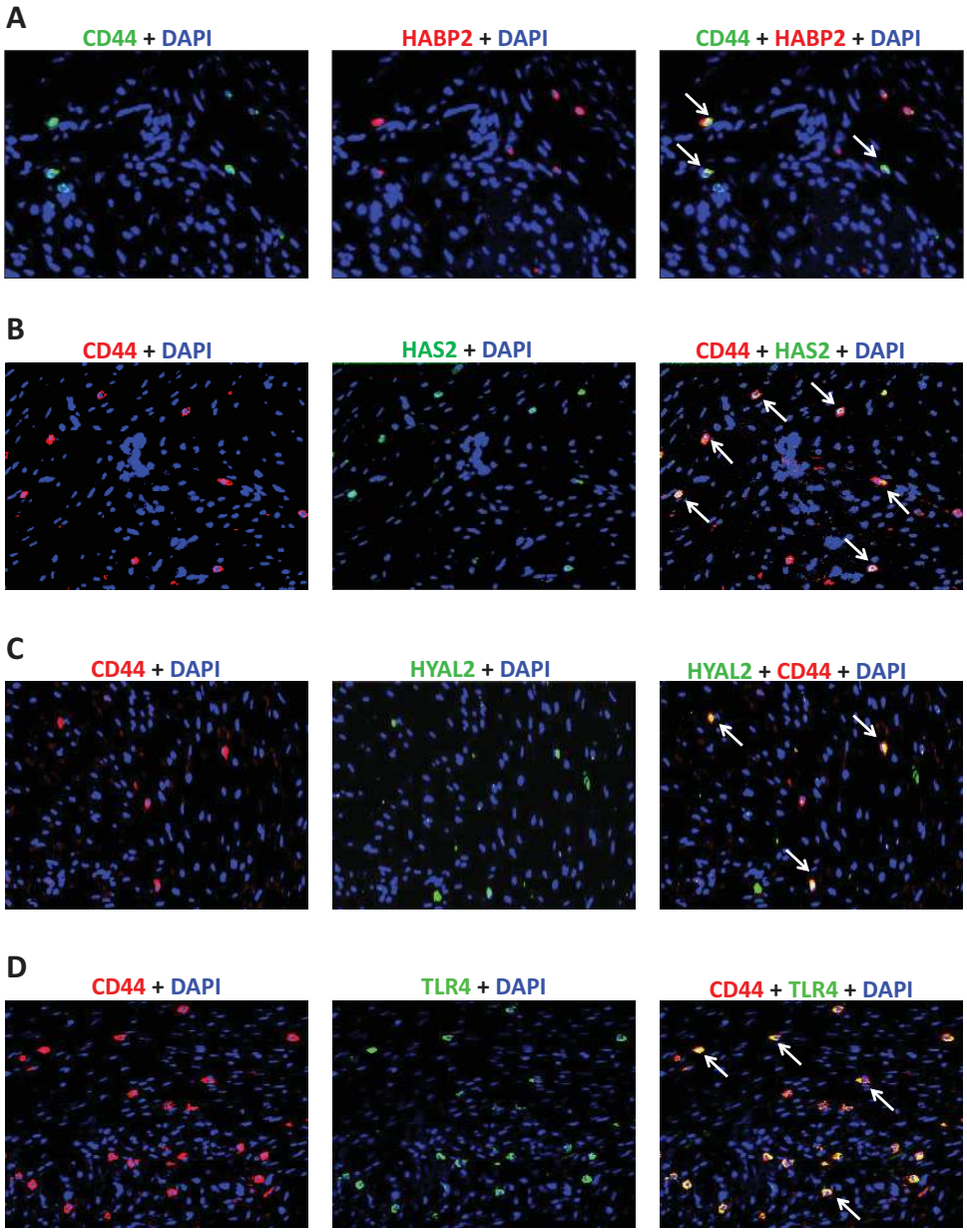

Figure 4. $CD44^+$ mesenchymal stem cells and HA crosstalk. (**A**) Fluorescent immunohistochemistry of paraffin-embedded DTs was performed and representative images showed coexpression of the mesenchymal stem cell marker CD44 and the HA binding protein, HABP2, (**B**) CD44 and the HA synthesizing protein, HAS2, (**C**) CD44 and the HA degrading protein, HYAL2, (**D**) and CD44 and the HA co-receptor, TLR4. Coexpression of both markers produced a yellow overlay indicated by white arrows. Nuclei were counterstained blue with DAPI. Images were taken at ×40 magnification.

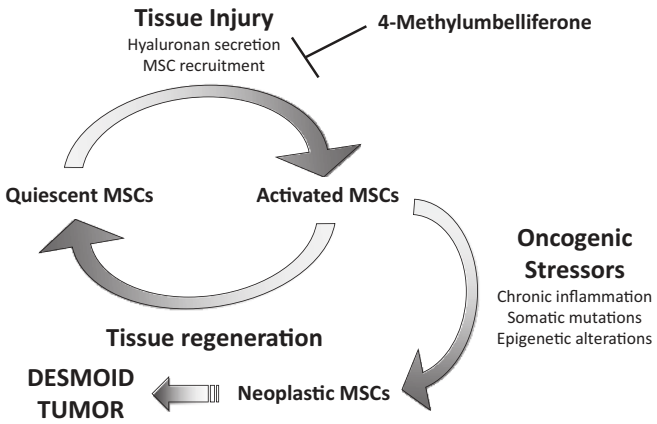

Figure 5. Schematic representation of DT etiology. Bone marrow-derived mesenchymal stem cells (MSCs) are recruited to sites of tissue injury in response to chemotactic signals, including HA. DTs may arise from activated MSCs with enhanced tumorigenic potential acquired during the proliferative phase of wound healing. Targeting HA-MSC interactions with 4-MU may offer a novel therapeutic approach for patients with DTs.

Here, we showed that HA and HAS2 expression was abundant in desmoid tissues as well as DT-derived cell lines (Figures 1 and 2). HYAL2 expression was similarly increased by ~2-fold in frozen desmoid tissues relative to normal controls, but this finding did not reach statistical significance (data not shown). Conversely, HA and HAS2 levels were low or absent in normal tissue and fibroblast controls. Prior studies demonstrated that HAS2 overexpression correlated with increased tumor cell proliferation and invasion *in vitro*, whereas inhibition of HA synthases decreased overall tumorigenicity, including metastatic disease, in a variety of tumor cell lines and animal models (30–33,36–40). In our studies, treatment with the HA inhibitor 4-MU effectively decreased HA and HAS2 levels as well as cellular proliferation in DT-derived cell lines (Figure 3). Consistent with our findings, Kosaki *et al.* showed that Has2 transfection in human HT1080 cells resulted in increased HA production, tumor cell proliferation, and tumor size in xenograft models (37). Similarly, Lokeshwar *et al.* found significant inhibition of prostate cancer cell proliferation, motility, and invasion following treatment with 4-MU (33). Taken together, our results suggest that HA metabolism may play a role in driving desmoid tumorigenesis and that future studies examining the antitumor effects of 4-MU, an orally available agent, in desmoid patients is warranted.

Bone marrow-derived MSCs are recruited to sites of tissue injury in response to inflammatory signals such as HA. Once engaged in its stem cell niche, activated MSCs may acquire somatic mutations or undergo epigenetic alterations during the proliferative phase of wound healing, resulting in enhanced tumorigenic potential (Figure 5). We hypothesize that DTs arise from such aberrantly activated MSCs that are unable to properly senesce or differentiate during the resolution phase of wound healing (20). MSC migration to injured tissue has been shown to depend upon CD44 cell surface expression and adhesion to HA (22,23). Downregulation of CD44 expression in breast cancer cells significantly inhibited HA-mediated chemotaxis following treatment with siRNA (41). In desmoid samples, we showed that MSCs expressed the major HA ligand CD44 as well as its coreceptor TLR4 (Figure 4). Interestingly, DTs in our library also showed ~2-fold increase in CD44 expression by quantitative PCR relative to normal tissue, although this upregulation was not statistically significant (data not shown). As such, HA-MSC interactions may play an important role in promoting CD44-dependent migration of bone marrow-derived MSCs to sites of tissue injury where DTs may arise as a result of unchecked wound healing.

In addition to chemotaxis, HA interactions with HA receptors such CD44 are responsible for initiating intracellular signaling events that regulate cell proliferation, migration, and apoptosis (42). Lokeshwar *et al.* (33) showed that mouse xenografts treated with oral 4-MU demonstrated decreased levels of CD44 and HAS2 expression and significant inhibition of PC3-ML tumor growth, primarily via inhibition of HA signaling. Tolg *et al.* (43) found that targeted deletion of receptor for HA-mediated motility (Rhamm), a HA co-receptor, attenuated the formation of DTs in an animal model of this disease. While we observed sparse Rhamm expression in our DT specimens (data not shown), we found abundant TLR4 staining of $CD44^+$ MSCs (Figure 4). TLR4 is a member of the toll-like receptor family that recognizes pathogens and activates the innate immune system. TLR4 also plays a role in noninfectious inflammation by forming a complex with CD44 and MD-2 to recognize HA (44). There is growing evidence to suggest that low-molecular weight HA promotes tumor proliferation, motility, and metastasis through TLR4 signaling (45–47). Inhibition of the CD44-TLR4-HA axis may be a novel therapeutic target for DTs and other solid tumors characterized by desmoplasia.

In conclusion, our studies demonstrate that HA is overexpressed in DTs and that 4-MU inhibition of HA synthesis significantly decreases proliferation in DT-derived cells. Furthermore, $CD44^+$ MSCs in DTs coexpress multiple members of the HA pathway including HA receptors and metabolizing/catabolizing proteins. Taken together, our results suggest that HA–CD44 interactions may contribute to desmoid tumorigenesis and that inhibition of HA signaling may offer a novel therapeutic approach to targeting the stromal microenvironment. Ultimately, new treatment strategies are needed that not only target differentiated fibroblasts comprising the tumor bulk, but also cancer stem cells and the tumor-stroma microenvironment, resulting in a more durable and complete response.

Funding

Desmoid Tumor Research Foundation, Inc. to N.L.C.

Acknowledgements

The authors thank Adelaide Carothers for her technical assistance and scientific guidance.

Conflict of Interest Statement: None declared.

References

1. Klemmer, S. et al. (1987) Occurrence of desmoids in patients with familial adenomatous polyposis of the colon. Am. J. Med. Genet., 28, 385–392.
2. Nichols, R.W. (1932) Desmoid tumors: a report of thirty-one cases. Arch. Surg., 7, 227–236.
3. Rodriguez-Bigas, M.A. et al. (1994) Desmoid tumors in patients with familial adenomatous polyposis. Cancer, 74, 1270–1274.
4. Hansmann, A. et al. (2004) High-dose tamoxifen and sulindac as first-line treatment for desmoid tumors. Cancer, 100, 612–620.
5. Mace, J. et al. (2002) Response of extraabdominal desmoid tumors to therapy with imatinib mesylate. Cancer, 95, 2373–2379.
6. Bertagnolli, M.M. et al. (2008) Multimodality treatment of mesenteric desmoid tumours. Eur. J. Cancer, 44, 2404–2410.
7. Gounder, M.M. et al. (2011) Activity of Sorafenib against desmoid tumor/deep fibromatosis. Clin. Cancer Res., 17, 4082–4090.
8. Mills, B.G. et al. (2000) Cytokines associated with the pathophysiology of aggressive fibromatosis. J. Orthop. Res., 18, 655–662.
9. Cheon, S.S. et al. (2002) beta-Catenin stabilization dysregulates mesenchymal cell proliferation, motility, and invasiveness and causes aggressive fibromatosis and hyperplastic cutaneous wounds. Proc. Natl. Acad. Sci. USA, 99, 6973–6978.
10. Dvorak, H.F. (1986) Tumors: wounds that do not heal. Similarities between tumor stroma generation and wound healing. N. Engl. J. Med., 315, 1650–1659.
11. Middleton, S.B. et al. (2000) Desmoids in familial adenomatous polyposis are monoclonal proliferations. Br. J. Cancer, 82, 827–832.
12. Li, M. et al. (1996) Desmoid fibromatosis is a clonal process. Hum. Pathol., 27, 939–943.
13. Stern, R. et al. (2006) Hyaluronan fragments: an information-rich system. Eur. J. Cell Biol., 85, 699–715.
14. Aruffo, A. et al. (1990) CD44 is the principal cell surface receptor for hyaluronate. Cell, 61, 1303–1313.
15. Naor, D. et al. (2002) CD44 in cancer. Crit. Rev. Clin. Lab. Sci., 39, 527–579.
16. Conget, P.A. et al. (1999) Phenotypical and functional properties of human bone marrow mesenchymal progenitor cells. J. Cell. Physiol., 181, 67–73.
17. Wu, Y. et al. (2007) Mesenchymal stem cells enhance wound healing through differentiation and angiogenesis. Stem Cells, 25, 2648–2659.
18. Fathke, C. et al. (2004) Contribution of bone marrow-derived cells to skin: collagen deposition and wound repair. Stem Cells, 22, 812–822.
19. Wang, G. et al. (2005) Adult stem cells from bone marrow stroma differentiate into airway epithelial cells: potential therapy for cystic fibrosis. Proc. Natl. Acad. Sci. USA, 102, 186–191.
20. Carothers, A.M. et al. (2012) Mesenchymal stromal cell mutations and wound healing contribute to the etiology of desmoid tumors. Cancer Res., 72, 346–355.
21. Wu, C. et al. (2010) Aggressive fibromatosis (desmoid tumor) is derived from mesenchymal progenitor cells. Cancer Res., 70, 7690–7698.
22. Herrera, M.B. et al. (2007) Exogenous mesenchymal stem cells localize to the kidney by means of CD44 following acute tubular injury. Kidney Int., 72, 430–441.
23. Zhu, H. et al. (2006) The role of the hyaluronan receptor CD44 in mesenchymal stem cell migration in the extracellular matrix. Stem Cells, 24, 928–935.
24. Weigl, P.H. et al. (1997) Hyaluronan synthases. J. Biol. Chem., 272, 13997–14000.
25. Stern, R. (2004) Hyaluronan catabolism: a new metabolic pathway. Eur. J. Cell Biol., 83, 317–325.
26. Volpi, N. et al. (2009) Role, metabolism, chemical modifications and applications of hyaluronan. Curr. Med. Chem., 16, 1718–1745.
27. Lokeshwar, V.B. et al. (2005) HYAL1 hyaluronidase: a molecular determinant of bladder tumor growth and invasion. Cancer Res., 65, 2243–2250.
28. Tammi, M.I. et al. (2002) Hyaluronan and homeostasis: a balancing act. J. Biol. Chem., 277, 4581–4584.
29. Turley, E.A. et al. (2002) Signaling properties of hyaluronan receptors. J. Biol. Chem., 277, 4589–4592.
30. Bharadwaj, A.G. et al. (2007) Inducible hyaluronan production reveals differential effects on prostate tumor cell growth and tumor angiogenesis. J. Biol. Chem., 282, 20561–20572.
31. Simpson, M.A. et al. (2002) Inhibition of prostate tumor cell hyaluronan synthesis impairs subcutaneous growth and vascularization in immunocompromised mice. Am. J. Pathol., 161, 849–857.
32. Li, Y. et al. (2007) Silencing of hyaluronan synthase 2 suppresses the malignant phenotype of invasive breast cancer cells. Int. J. Cancer, 120, 2557–2567.
33. Lokeshwar, W.B. et al. (2010) Antitumor activity of hyaluronan synthesis inhibitor 4-methylumbelliferone in prostate cancer cells. Cancer Res., 70, 2613–2623.
34. Vigetti, D. et al. (2009) The effects of 4-methylumbelliferone on hyaluronan synthesis, MMP2 activity, proliferation, and motility of human aortic smooth muscle cells. Glycobiology, 19, 537–546.
35. Kakizaki, I. et al. (2004) A novel mechanism for the inhibition of hyaluronan biosynthesis by 4-methylumbelliferone. J. Biol. Chem., 279, 33281–33289.
36. Whatcott, C.J. et al. (2011) Targeting the tumor microenvironment in cancer: why hyaluronidase deserves a second look. Cancer Discov., 1, 291–296.
37. Kosaki, R. et al. (1999) Overproduction of hyaluronan by expression of the hyaluronan synthase Has2 enhances anchorage-independent growth and tumorigenicity. Cancer Res., 59, 1141–1145.
38. Udabage, L. et al. (2005) The over-expression of HAS2, Hyal-2 and CD44 is implicated in the invasiveness of breast cancer. Exp. Cell Res., 310, 205–217.
39. Yoshihara, S. et al. (2005) A hyaluronan synthase suppressor, 4-methylumbelliferone, inhibits liver metastasis of melanoma cells. FEBS Lett., 579, 2722–2726.
40. Okuda, H. et al. (2012) Hyaluronan synthase HAS2 promotes tumor progression in bone by stimulating the interaction of breast cancer stem-like cells with macrophages and stromal cells. Cancer Res., 72, 537–547.
41. Tzircotis, G. et al. (2005) Chemotaxis towards hyaluronan is dependent on CD44 expression and modulated by cell type variation in CD44-hyaluronan binding. J. Cell Sci., 118(Pt 21), 5119–5128.
42. Sironen, R.K. et al. (2011) Hyaluronan in human malignancies. Exp. Cell Res., 317, 383–391.
43. Tolg, C. et al. (2003) Genetic deletion of receptor for hyaluronan-mediated motility (Rhamm) attenuates the formation of aggressive fibromatosis (desmoid tumor). Oncogene, 22, 6873–6882.
44. Taylor, K.R. et al. (2007) Recognition of hyaluronan released in sterile injury involves a unique receptor complex dependent on Toll-like receptor 4, CD44, and MD-2. J. Biol. Chem., 282, 18265–18275.
45. Dang, S. et al. (2013) Stimulation of TLR4 by LMW-HA induces metastasis in human papillary thyroid carcinoma through CXCR7. Clin. Dev. Immunol. Epub 2 December 2013.
46. Wu, Y. et al. (2011) Neutrophils promote motility of cancer cells via a hyaluronan-mediated TLR4/PI3K activation loop. J. Pathol., 225, 438–447.
47. Jiang, D. et al. (2011) Hyaluronan as an immune regulator in human diseases. Physiol. Rev., 91, 221–264.